

# Fuzzy Logic Based FOGI-FLL Algorithm for Power quality improvement with Recursive Digital Filter Based Control of a Grid Tied Solar PV System

D. Anusha, B.Tech. Student, EEE Department, Chadalawada Ramanamma Engineering College, Tirupati, Andhra Pradesh, India, aanu43137@gmail.com

Dr. J. Srinu Naick, Professor, EEE Department, Chadalawada Ramanamma Engineering College, Tirupati, Andhra Pradesh, India, speaksrinu@gmail.com

**Abstract** —This paper presents a control approach to the transfer of active power between the solar photovoltaic (PV) and grid / loading array - with increased power quality by removing harmonics and providing reactive power compensation needed by the load on the distribution network. The proposed method to improve the performance of the fourth-based fuzzy logic system based on general integrator (FOGI) frequency-based control (FLL) for optimal operation of the solar energy conversion system (SECS) has the distribution capability of static compensator (DSTATCOM) along with supplying active power to the distribution network. Fogi-FLL has a higher ordering ability than conventional algorithms. When compared to traditional algorithms, the proposed control technique's frequency tracking capacity outperforms them. The recursive digital filter control is used to increase the PQ index of the Interfaced Grid PV system by functioning all of the time and assuring power flows between network utilities and linked loads. Recursive digital filters are used to process load currents and extract the active power components of them. The prototype system was developed in the laboratory and its performance was studied for various charges, changing solar insulating, and swelling voltage, conditions of voltage and voltage distortion.

**Keywords** — *Distribution Static Compensator (DSTATCOM), Fuzzy Logic, Maximum Power Point, Power Quality, Recursive Digital Filter, Solar PV Generation.*

## I. INTRODUCTION

The issues with the usage of fuels are the prime highlight of Paris Climate Agreement in 2015, wherever the reduction within the usage of fossil fuel primarily based energy sources, has been stressed. Because the electricity obtained from renewable energy sources [1] has no result on the greenhouse gas emissions, it's termed as inexperienced power and is obtained commercially from solar, wind, biomass, geothermic and hydro energy sources. Their demand will be attributed to the requirement for minimization of carbonic acid gas emission and therefore the usage of oil. The usage of renewable energy, is being emphasized thanks to the alarming levels of pollution created by standard energy resources. The renewable energy sources being exploited embrace solar power, wind energy, periodic event energy and bio-mass energy. The distributed generations (DGs) are centered on the usage of renewable energy sources, as they are doing not manufacture pollution, they're clean kind of energy and are found in abundance in

nature [2]. The demand for exploitation of star energy, is increasing, with a rise within the government subsidies. The harnessing of solar energy is gaining popularity, because it is accessible in abundance and therefore the solar power plants aren't recognized of any moving parts. Among the quickest growing distributed energy sources is that distributed energy sources is the solar photovoltaic distributed generation (PV-DG) system thanks to the extensive offer of solar energy and therefore the easy installation. The rationale of utilizing PV power in distribution network in place of usage within the transmission grid is primarily in regard with the regulative and economic factors.

The PV-DG system considerably affects the power quality (PQ) [3] and system operation because of intermittent convenience of star PV power caused by severe weather conditions. The first constituent of solar PV system is PV arrays, within which the link of solar PV current and voltage is nonlinear resulting in problems in utilization of most power. So as to force the solar PV system to control at

maximum power point (MPP) in any respect environmental conditions, techniques are recognized as maximum power point trailing techniques (MPPT). in depth analysis has been according within the literature as MPPT is an important a part of a PV system. Because of reduced complexness and easy implementation, perturb and observe (P&O) technique is utilized. The widespread adoption of alternative energy generation [4-5] poses difficulties in steady-state and transient operation for problems like weather-induced changes in generation, voltage unbalances and protecting devices. the first reason for the rise in usage of grid connected PV system, is in regard with storage of excess power into the grid thereby minimizing the need of large and expensive batteries. This becomes attainable if sunshine is on the market in plenty, thus, internet power outflow to the grid are often achieved with native star generation [6] that causes a discount within the internet demand on a distribution feeder. However, the accumulated penetration of PV-DG system to the utility grid, ends up in enhanced challenges in regard with the system operator and utilities. The intermittent nature of alternative energy needs the usage of energy storage, which may be classified as grid interfaced solar PV system or standalone solar PV system [7-8]. the recognition of grid connected system are often attributed to the non-utilization of the battery for energy storage. The increasing inclination towards grid connected system is because of the usage of the grid for storage purposes, thereby up the performance by reducing complexness and value of the system. Among the single-stage and double stage utilization of grid connected systems, single stage topologies are useful because of reduction in cost and reduce in losses [9]. Moreover, the employment of VSC is important as power cannot be fed directly into the grid and so at the purpose of intersection (PIC), the star PV array is connected to the grid through VSC. At the PIC wherever the load and grid are connected, there is variety of things inflicting power quality (PQ) deterioration [10]. Due to these, harmonics and disturbances are determined with reference to the connected nonlinear loads. In addition, PQ problems arise because of below voltage and over voltage conditions that cause loss of important information and cost. Thus, VSC performs distribution static compensator operation, to boost the availability reactive power and power factor. So as to handle these PQ issues, many management algorithms [11-13] are present in the literature cherish instant reactive power theory [14], section barred loop based mostly control algorithms and least mean square (LMS) based control algorithms [15]. the key disadvantage with the adjective LMS control technique is in regard with the degradation in performance because of formatting error and noise determined within the signaling power. Moreover, the accuracy is hampered due to variable input characteristics. Moreover, the generalized algorithms and therefore the

improved linear curving tracer (ILST) [16] also are according in the literature however their performance isn't reported below weak grid conditions. In addition, the model predictive controller (MPC) is being used today but it possesses the key disadvantage in terms of complexity. Moreover, the phase locked loops (PLLs) control techniques [17] such as fixed frequency PLL (FFPLL), quadrature PLL (QPLL) and synchronous reference frame (SRF-PLL) exist within the literature, however the presence of abc/dq transformation enhances their complexness and deteriorates the dynamic behavior in conjunction with a rise in the machine burden. These techniques also observe sluggish response because of the inherent transformations needed throughout their application. Moreover, the key disadvantage is set with second order generalized integrator (SOGI) in terms of DC offset [18] primarily based management algorithms and thus the presence of fourth order improvement in least mean fourth (LMF) management techniques, leads to steady state performance degradation. In addition, the distinct Fourier transform (DFT) [19] techniques also are current in the literature however they suffer because of asynchronous sampling, that successively affects the grid synchronization due to the presence of section errors. The complexness issue additionally arises with back propagation (BP) [20-21] management techniques as they need a coaching mechanism so as to handle the hidden layers. Therefore, the algorithmic digital filter has been used during this paper to boost performance throughout weak grid conditions because it has ne'er been enforced before. The recursive digital filter control technique uses indirect current control mechanism by determinant the elemental load current in order to work out the grid currents [22-23]. Consequently, it determines the grid currents and therefore the major advantage of this management lies within the speedy extraction with reduced complexness of load active power component. Moreover, the additional benefit obtained, is in terms of reduced price with accumulated efficiency. the key contribution of this paper, are non-commissioned as follows. The recursive digital filter is used during this work for the economic management of grid tied solar PV system as this application of recursive digital filter has ne'er been implemented before.

- The satisfactory operation is ascertained throughout weak grid conditions as evident from the experimental validation for various check conditions of load unbalancing, voltage sag, voltage distortion, voltage swell and dynamic solar irradiation conditions.
- The advance in dynamic response is achieved by the usage of PV feed-forward term within the control technique so as to boost the speed of operation of the recursive digital filter management technique.
- The system performable has additionally been valid in agreement with the IEEE-519 customary and therefore

the total harmonic distortion of the grid currents, is ascertained to lower than 5%.

## II. SYSTEM CONFIGURATION

The schematic diagram of the system is conferred in Fig.1 wherever power to the nonlinear loads, is fed by one stage PV array and therefore the utility grid. The PV array is connected across the VSC and feeds excess power to the grid for the storage. The distribution static compensator (DSTATCOM) operation of VSC is performed at the point of intersection (PIC) by feeding compensating currents and so eliminating harmonics and up the power quality. Thus, the management technique is distinguished for the right injection of compensating currents that relies upon the satisfactory determination of reference currents. Throughout this process, for reducing these ripples within the compensating currents, interfacing inductors ( $L_f$ ) are utilized. Subsequently, the switching ripples are removed by the utilization of ripple filters ( $R_f$  and  $C_f$ ), that alleviates their impact at PIC. With the usage of current and voltage sensors, the voltage of DC link ( $V_{dc}$ ), load currents ( $i_{La}$ ,  $i_{Lb}$ ), grid voltages ( $v_{ab}$ ,  $v_{bc}$ ), grid currents ( $i_{sa}$ ,  $i_{sb}$ ), and PV current ( $I_{pv}$ ) are detected for manufacturing the switching pulses of VSC. The management structure utilized here, consists of a algorithmic digital filter (Fig. 2) which alleviates harmonics in the system. It performs satisfactory twin mode operation throughout the day and therefore the utilised system parameters are given in Appendix.

### III. CONTROL TECHNIQUE

The control structure utilizing recursive digital filter is explained in the following section. Fig. 2 shows the control mechanism in which appropriate VSC switching is performed by obtaining reference currents ( $i_{sa}^*$ ,  $i_{sb}^*$ ,  $i_{sc}^*$ ) with proper estimation of grid voltages ( $v_{sa}$ ,  $v_{sb}$ ,  $v_{sc}$ ), grid currents ( $i_{sa}$ ,  $i_{sb}$ ,  $i_{sc}$ ) and unit templates ( $u_{pa}$ ,  $u_{pb}$ ,  $u_{pc}$ ).

### A. Variable Step Size Perturb and Observe for Improving Performance under Partial Shading Conditions

The perturb and observe (P&O) maximum power point technique is preferred because it is simple to use and implement. However, oscillations around the maximum power point (MPP) and slow reaction during changeable insulation circumstances, particularly partial shade conditions, show a decline in performance. As a result, variable step size P&O MPPT [24-25] is used, with the main benefit of automatic step size tuning during changes in solar insulation conditions. When a step change in solar irradiation occurs, the tuning of step size is achieved, according to the operational point. When the operational point is far from MPP, the ability to track quickly is gained by increasing the step size. The problem is solved by using

a variable step size P&O MPPT, in which the performance is dictated by the scaling factor  $N$ , ensuring that the system performs well under different solar insulation circumstances.

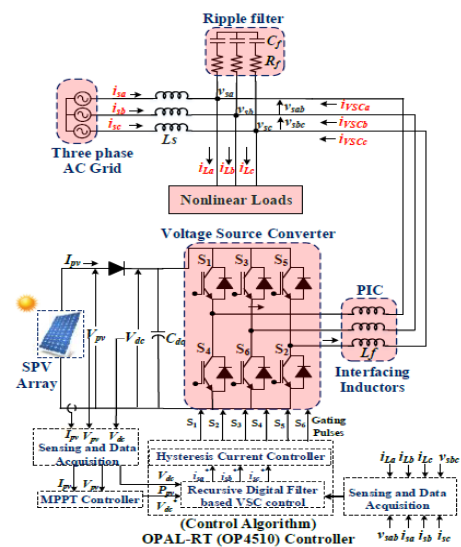


**Fig. 1 System configuration.**

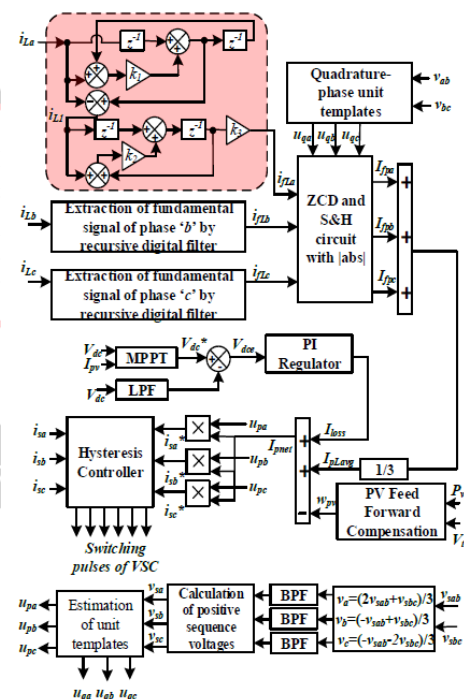


**Fig.2 Control technique based on recursive digital filter.**

$$V_k^* = V_k - N \frac{\Delta P}{\Delta I} \quad (1)$$

### B. Calculation of Unit Templates (In-Phase and Quadrature- Phase)

The phase voltages of the grid are determined from the line voltages [26],

$$\begin{aligned} v_a &= (2v_{sab} + v_{sbc})/3, \\ v_b &= (-v_{sab} + v_{sbc})/3, \\ v_c &= (-v_{sab} - 2v_{sbc})/3 \end{aligned} \quad (2)$$

In order to tackle the issues of voltage unbalance a recursive digital filter is utilized as band-pass filter [27] in order to extract the  $v_{sa}$ ,  $v_{sb}$ ,  $v_{sc}$  components. These are further utilized for the estimation of the terminal voltage ( $V_t$ ),

$$V_t = \sqrt{\frac{2(v_{sa}^2 + v_{sb}^2 + v_{sc}^2)}{3}} \quad (3)$$

Therefore, the in-phase and quadrature phase unit templates are obtained from  $V_t$  and  $v_{sa}$ ,  $v_{sb}$ ,  $v_{sc}$ ,

$$u_{pa} = \frac{v_{sa}}{V_t}, \quad u_{pb} = \frac{v_{sb}}{V_t}, \quad u_{pc} = \frac{v_{sc}}{V_t} \quad (4)$$

$$u_{qa} = \frac{(-u_{pb} + u_{pc})}{\sqrt{3}}, \quad u_{qb} = \frac{(3u_{pa} + u_{pb} - u_{pc})}{2\sqrt{3}}, \quad u_{qc} = \frac{(-3u_{pa} + u_{pb} - u_{pc})}{2\sqrt{3}} \quad (5)$$

### C. Utilization of Recursive Digital Filter

Recursive digital filters are a type of variable digital filter (VDF) that determines the cut-off frequency ( $f_c$ ) with minimal complexity and fewer parameters. Every unit delay is replaced with an all-pass structure in the digital filter. The  $i_{La}$  is estimated by recursive digital filter using change in coefficients and proper use of recursive digital filter. The filter is made up of delays with low pass characteristics, making it simple to regulate. The system's performance is improved by reducing the number of parameters involved in the execution. Furthermore, the filter parameters are calculated based on the system requirements. They are obtained by building a prototype filter with  $f_{c0}$  as the cut-off frequency and  $A(z)$  as the unit delay replacement. The intermediate signal of  $i_{L1}$ , calculated as, can reveal the  $A(z)$ .

$$A(z) = \frac{i_{L1}}{i_{La}} = \frac{-k_1 + z^{-1}}{1 - k_1 z^{-1}} \quad (6)$$

Thus,  $f_{ca}$  (cut-off frequency) changes by varying  $k_1$  and  $k_2$ .

In order to set the gains of the recursive filter, the mathematical relation between the existing cut-off frequency  $\omega_{c0} = 2\pi f_{c0}$ , desired cut-off frequency  $\omega_{ca} = 2\pi f_{ca}$ , decimation factor ( $M$ ) and the filter gains ( $k_i$ ) is utilized [23]. For a causal filter the phase and frequency responses are given as,

$$\theta_c(\omega) = -\omega - 2 \tan^{-1} \left[ \frac{\alpha \sin \omega}{1 - \alpha \cos \omega} \right] \quad (7)$$

$$A(e^{j\omega}) = \frac{-\alpha + e^{-j\omega}}{1 - \alpha e^{-j\omega}} \quad (8)$$

Moreover, for  $A(z)$ , the phase delay  $\tau_p(\omega)$  is,

$$\tau_p(\omega) = \frac{-\theta_c(\omega)}{\omega} = 1 + \frac{2}{\omega} \tan^{-1} \left[ \frac{\alpha \sin \omega}{1 - \alpha \cos \omega} \right] \quad (12)$$

The decimation factor ( $M$ ) and  $\omega_{c0}$ ,  $\omega_{ca}$  are related according to the following equation,

$$\omega_{ca} = \frac{\omega_{c0}}{\tau_p(\omega_{ca})} \times M \quad (9)$$

$$\omega_{c0} = \frac{\omega_{ca}}{M} + \frac{2}{M} \tan^{-1} \left[ \frac{\alpha \sin \omega_{ca}}{1 - \alpha \cos \omega_{ca}} \right] \quad (10)$$

Therefore, as observed from algebraic simplification,

$$\alpha = \left[ \frac{\tan x}{\sin \omega_{ca} + \tan x \times \cos \omega_{ca}} \right] \quad (11)$$

where,

$$x = \frac{M\omega_{c0} - \omega_{ca}}{2} \quad (12)$$

Thus, in order to obtain the desired  $\omega_{ca} = 2\pi f_{ca}$ , the value of gains are calculated and the value of centre frequency  $f_{center}$  is determined in the similar manner in order to obtain band-pass response as,

$$k_i = -\cos(f_{center} \times \pi) \quad (13)$$

Therefore, the transfer function representing relation between  $i_{La}$  and  $i_{L1}$  is given as [23],

$$\frac{i_{L1}}{i_{La}} = k_3 \left( \frac{-k_1 + z^{-1}}{1 - k_1 z^{-1}} \right) \left( \frac{-k_2 + z^{-1}}{1 - k_2 z^{-1}} \right) = \frac{k_3 k_2 k_1 - k_3 k_2 z^{-1} - k_3 k_1 z^{-1} + k_3 z^{-2}}{1 - k_1 z^{-1} - k_2 z^{-1} + k_1 k_2 z^{-2}} \quad (14)$$

The major objective of the recursive digital filter lies in the quick convergence in obtaining the component of active power ( $I_{pa}$ ). The  $i_{La}$  acquired is passed through zero crossing detector (ZCD), which is also provided with ( $u_{qa}$ ,  $u_{qb}$ ,  $u_{qc}$ ). Consequently, after passing through the absolute block, load current fundamental ( $I_{pa}$ ) component is obtained. Similarly,  $I_{pb}$  and  $I_{pc}$  are determined and the average of load currents fundamental ( $I_{pa}$ ,  $I_{pb}$ ,  $I_{pc}$ ) component is estimated as,

$$I_{pLav} = (I_{pa} + I_{pb} + I_{pc}) / 3 \quad (15)$$

The  $V_{dce}$  is obtained from  $V_{dc}$  and  $V_{dc}^*$ ,

$$V_{dce} = V_{dc}^* (m) - V_{dc} (m) \quad (16)$$

This is utilized to obtain the DC loss component with the help of a proportional-integral (PI) controller.

$$I_{loss} (m) = K_p \{V_{dce} (m)\} + K_i \{V_{dce} (m) - V_{dce} (m-1)\} + I_{loss} (m-1) \quad (17)$$

### D. Determination of the PV Feed-Forward Term

The calculation of PV feed-forward term is performed by dividing the solar PV power and the terminal voltage as,

$$w_{pv} = (2P_v) / (3V_t) \quad (18)$$

where,  $P_v$ ,  $V_t$  denote the power obtained from PV array and terminal voltage, respectively. The grid active power component is obtained from  $I_{pLav}$ ,  $I_{loss}$  and  $w_{pv}$  as,

$$I_{pnet} = I_{pLav} + I_{loss} - w_{pv} \quad (19)$$

### E. Evaluation of Reference Grid Currents and Switching of VSC

The multiplication of  $I_{pnet}$  with the respective in-phase unit template ( $u_{pa}$ ,  $u_{pb}$ ,  $u_{pc}$ ) is performed to determine the reference currents,

$$i_{sa}^* = I_{pnet} \times u_{pa}, \quad i_{sb}^* = I_{pnet} \times u_{pb}, \quad i_{sc}^* = I_{pnet} \times u_{pc} \quad (20)$$

For determining VSC switching, the hysteresis current controller is supplied with the difference between actual and reference grid currents presented as,

$$i_{esa} = i_{sa}^* - i_{sa}, \quad i_{esb} = i_{sb}^* - i_{sb}, \quad i_{esc} = i_{sc}^* - i_{sc} \quad (21)$$

For the protection of VSC switches, a limiting method for current is utilized in order to determine the reactive power (Q) [28]. The ( $v_{p\alpha}$ ,  $v_{p\beta}$ ,  $v_{n\alpha}$ ,  $v_{n\beta}$ ) are the positive and negative sequence components which are computed as,

$$\begin{bmatrix} v_{p\alpha} \\ v_{p\beta} \end{bmatrix} = \sqrt{\frac{1}{6}} \begin{bmatrix} 1 & -e^{-j\pi/2} \\ e^{-j\pi/2} & 1 \end{bmatrix} \begin{bmatrix} v_{sa} \\ v_{sb} \\ v_{sc} \end{bmatrix} \quad (22)$$

$$V_p = \sqrt{v_{p\alpha}^2 + v_{p\beta}^2}, \quad V_n = \sqrt{v_{n\alpha}^2 + v_{n\beta}^2} \quad (23)$$

Here, the magnitude of positive and negative sequence components are denoted by  $V_p$  and  $V_n$  and thus, the calculation of reactive power is achieved as,

$$Q = \begin{cases} 0 & (V_{pu} > 0.9) \\ (0.9 - V_{pu}) \times S \times 1.5 & (V_{pu} \text{ between } 0.2, 0.9) \\ S \times 1.05 & (V_{pu} < 0.2) \end{cases} \quad (24)$$

where,

$$V_{pu} = \sqrt{v_p^2 + v_n^2} / V_{base} \quad (25)$$

Depending on the depth in grid voltage, the different patterns for reactive power supply are presented as,

Reactive power supplied is zero if depth is less than 0.1 pu.

The reactive power is given as  $1.5 \times \square \times (0.9 - \square\square\square)$ , for depth between (0.1 pu, 0.8 pu). Moreover, Q is estimated to be  $1.05 \times$  inverter rating, if depth is more than 0.9. Thus, these computations are utilized for the satisfactory operation of VSC switches.

### F. Comparative Performance

In terms of performance, the recursive digital filter is compared to traditional control approaches in Figure 3. The recursive digital filter's better performance may be seen in the fact that it gives accurate estimation with no oscillations and a significantly faster convergence rate. The adaptive least mean fourth (LMF) control approach has erroneous steady state performance, as well as a low notch filter convergence rate. As a result, the recursive digital filter provides satisfactory performance and quick reaction. In addition, a comparison of the recursive digital filter to various control algorithms is presented in Table I.

TABLE I. COMPARATIVE PERFORMANCE

Parameters	SOGI-FLL	SRFT-PLL	Recursive digital filter
PLL requirement	No	Yes	No
THDs in grid current	4%	4.3%	3.4%
Oscillation in amplitude estimation	(2*DC offset)	2 to 5 A	0 A
Computational burden	0.62 ms	3.94 ms	0.224 ms
Complexity	Medium	High	Low

## IV. DEVELOPING CONTROL FOR THE NEW SCHEME

### A. Design Procedure for FOGI Block

The gains K1 and K2 are critical for extracting the fundamental component from the load current's non-sinusoidal non-sinusoidal component. In the literature, the process for tweaking gains in a generalised integrator is outlined [29-30].

### B. Structure of Frequency Locked Loop

The frequency locked loop is used to track the frequency of the system. The basic three stages in the design of fuzzy logic control are fuzzification, fuzzy control rules, and defuzzification. Measurement of inputs and setting up rules are used to achieve fuzzification and fuzzy control rules, respectively. Defuzzification is the process of transforming rules to produce the output signal.

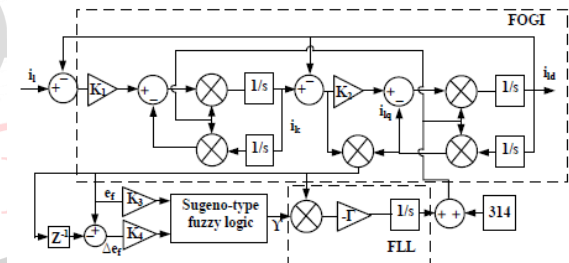


Fig.3. Detail scheme of fuzzy logic controller based FOGI-FLL

Takagi-Sugeno fuzzy logic controller receives error signal and rate of variation in error signal as inputs. The shape of a fuzzy set is frequently decided by the system and can be determined by the system's knowledge and control problem. The linguistic rules are achieved in a variety of ways depending on the parameters. The Takagi-Sugeno fuzzy logic controller can solve a wide range of nonlinear control problems more effectively. The Takagi-Sugeno fuzzy logic controller is used to track system frequency and deliver gains. The process for designing membership functions can be found in the literature [31]. A nonlinear function of frequency and its derivative is the frequency error. As a result, the fuzzy logic controller uses frequency error and the rate of fluctuation in frequency error as input variables. The fuzzy logic controller is used to tune gain Y. Fig. 4 depicts membership relation for input and outputs. The MP (More Positive), LP (Less Positive), Z (Zero), LN

(Less Negative), MN (More Negative), B (Big), M (Medium), L (Little) are linguistic variables, which are membership functions for fuzzy set input and output. The grade of member ship function, is obtained from,

$$\mu(x)=1-|x-m|/(0.5w) \quad (26)$$

where, w, m and x, are width and coordinate of the point at which grade of member function, is one and input variable respectively. Here Sugeno-type fuzzy logic controller with inference mechanism is used. The weighting factor  $W_t$  is used to give weight to the each rules. The minimum operation is evaluated as,

$$w_i = \min \{ \mu_{FR\_Error}(F), \mu_{FR\_Error}(\Delta F) \} \quad (27)$$

The average weight of all outputs is assessed using the variation of integral gain (Igain), which is calculated as, where N and  $C_i$  are the total number of rules and ordinates corresponding to the respective consequent membership function, respectively.

$$I_{gain} = \sum_{i=1}^N w_i C_i / \sum_{i=1}^N w_i \quad (28)$$

Rule: if mistake is  $A_i$  and change in error is  $B_i$ , then Igain is  $C_i$  is the fuzzy rule. A and B are fuzzy subsets, but  $C_i$  is a singleton. The collection of fuzzy rules is listed in Table II. Table II describes the mistake in frequency fuzzification method. For simplicity, the fuzzy logic controller's inputs are scaled down by 1000, which is dependent on the frequency error fluctuation. The design approach is illustrated as follows in order to create fuzzy logic controller rules (see Table II). The dynamics of the FLC inputs are shown in Figs. 5 and 6 when the system frequency varies from 50Hz to 51Hz at 0.5s (a-b). The fluctuation in both FLC inputs with its varied zones is depicted in Fig. 5 (a). Figure 5 shows the phase plane analysis of the FLC inputs (b). Table II shows how the rules in Table I are based on the FLC inputs' areas. When the frequency of the system changes,  $e_f$  and  $e_f$  climb higher than 500 and 5 in the transitory condition. As FLL tracked the system frequency, both FLC inputs  $e_f$  and  $e_f$  were lowered to zero. During high FLC input jumps, the minimum value (low (L)) should provide the smallest multiplying factor and provide the most damping. As a result, in the estimation of the system frequency, there are few or no oscillations. The low (L) output gain value aids in the mitigation of excessive transient. Under transitory conditions, the second input also falls in the MP area, as illustrated in Fig. 5. (b). As a result, if both inputs are in the MP range, the output gain should be low (L) to ensure enough damping during smooth dynamic performance. As a result, in Table II, the last column (MP) corresponding to the first FLC input ( $e_f$ ) and the last row (MP) relating to the

second FLC input ( $e_f$ ) have low values (L). It's the same for the column that corresponds to LN for the first FLC input ( $e_f$ ) and the column that corresponds to LN for the second FLC input ( $e_f$ ). When the system frequency is reduced, FLC must give the least gain for proper damping because both FLC inputs leap to the negative direction. The low (L) gain and big (B) gain, help to damp input oscillations and to reach steady-state quickly. Therefore, output gain is big (B) for the scenario where one or both inputs of FLC fall in Z region. Moreover, big (B) gain is required when one or both of FLC inputs fall under P and N regions to facilitate quickly tracking of estimated frequency in steady-state. However, when one of the inputs of FLC, falls in Z region and other falls in LP and LN regions,

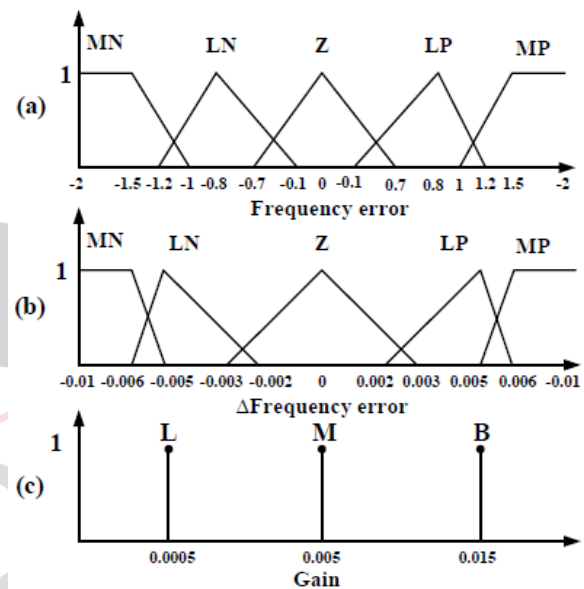


Fig.4. Membership functions (a) Frequency error (b) variation in frequency error (c) Internal gain (Igain)

TABLE II RULES FOR FUZZY LOGIC CONTROLLER

		$e_f$				
$\Delta e_f$		MN	LN	Z	LP	MP
	MN	L	L	L	L	L
	LN	L	B	M	B	L
	Z	L	M	B	M	L
	LP	L	B	M	B	L
	MP	L	L	L	L	L

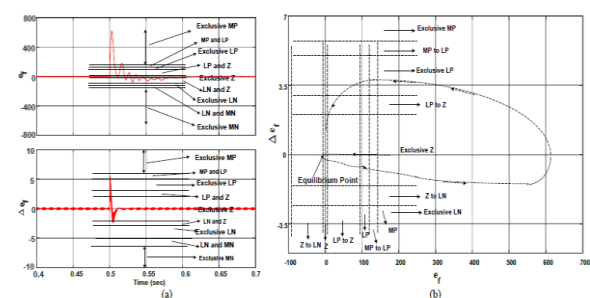


Fig.5. Trajectory of the fuzzy input-1 ( $e_f$ ) and change in error fuzzy input-2 ( $\Delta e_f$ )

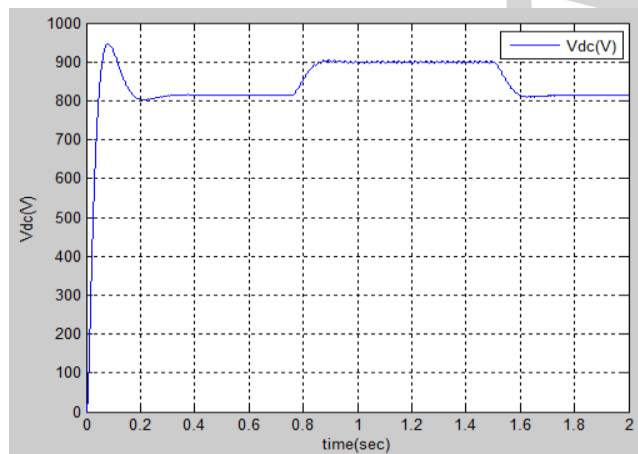
oscillations are likely to happen in estimated system frequency in steady-state condition. Hence, it is always safe to keep medium (M) gain to mitigate oscillations even after reaching steady-state value. Thus, all the entries in Table II, are covered hereby and corresponding entries are justified.

## V. SIMULATION RESULTS

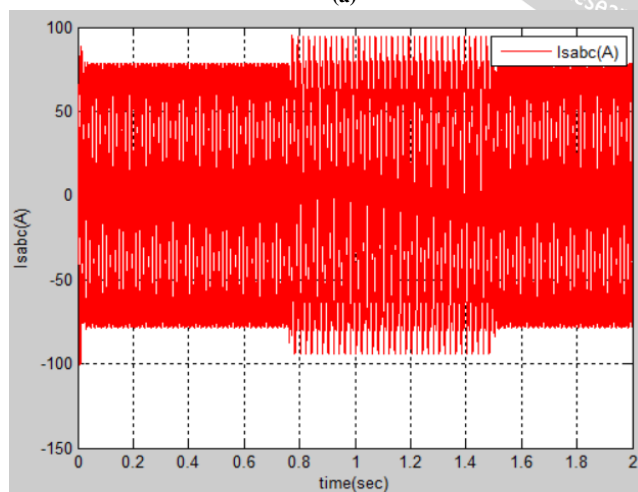
The simulation of recursive digital filter is performed and analysed using MATLAB/SIMULINK software for different conditions as presented in this section. Various parameters such as load currents ( $i_{Labc}$ ), grid currents ( $i_{sabc}$ ), grid voltages ( $v_{sabc}$ ), solar PV parameters and control signals are observed. The satisfactory performance is shown here for various dynamic and steady-state conditions such as variable insolation and dynamic loading.

### A. Dynamic Loading Condition

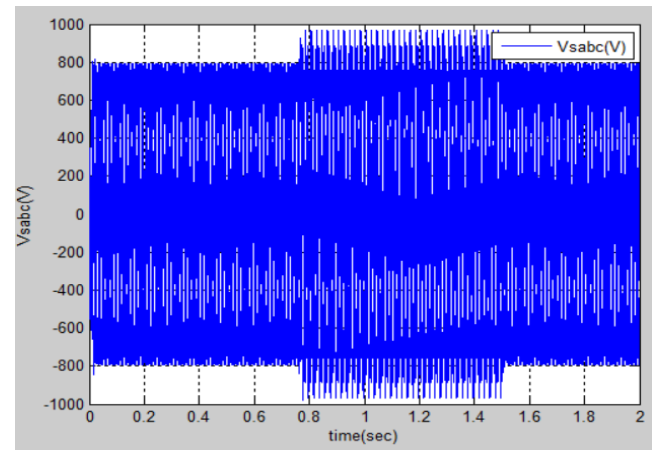
The dynamic loading condition is witnessed due to disconnection or addition of a phase load suddenly. For the purpose of verification of performance during this condition,



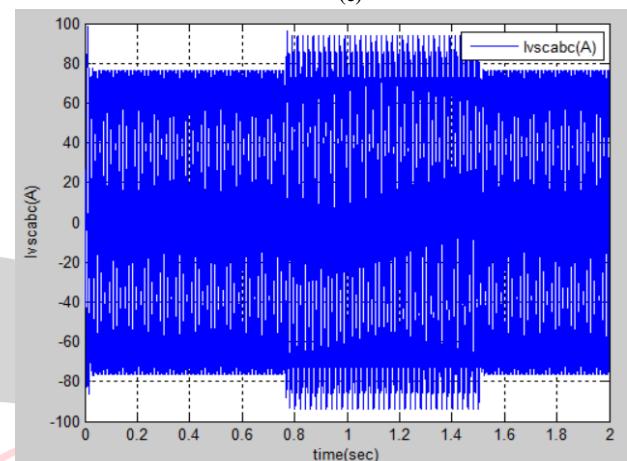
(a)



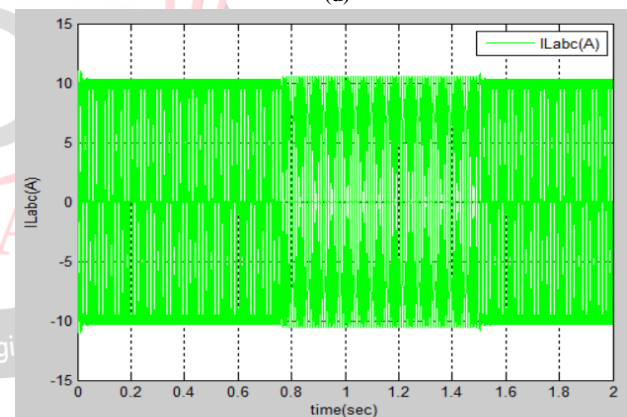
(b)



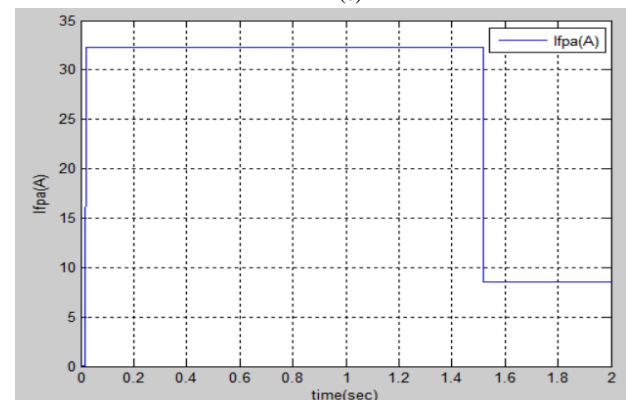
(c)



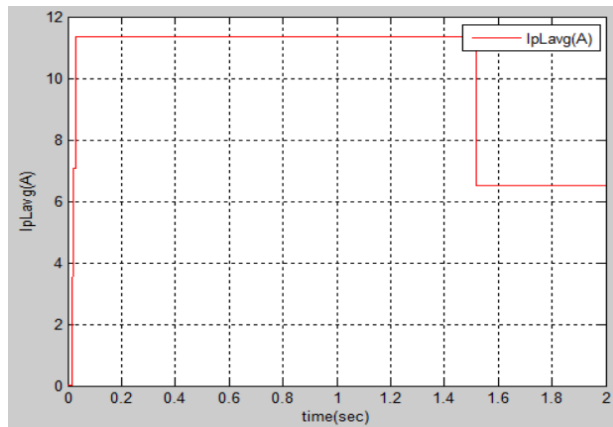
(d)



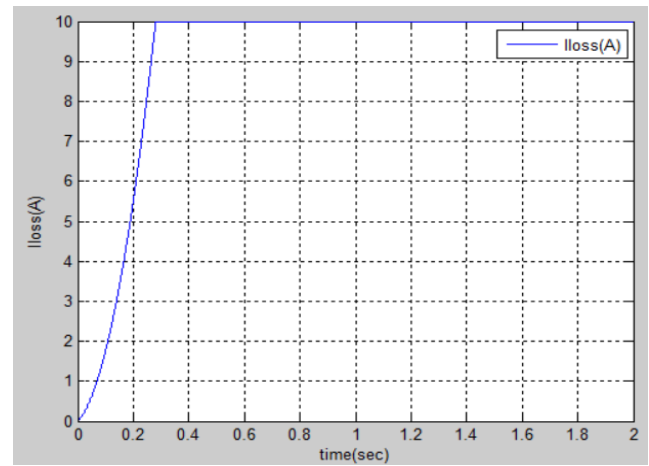
(e)



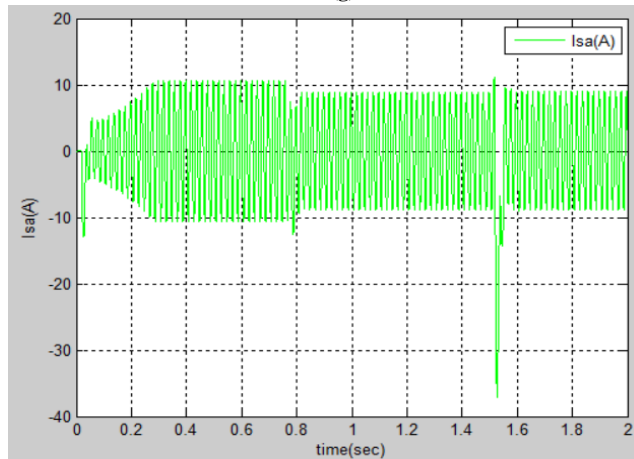
(f)



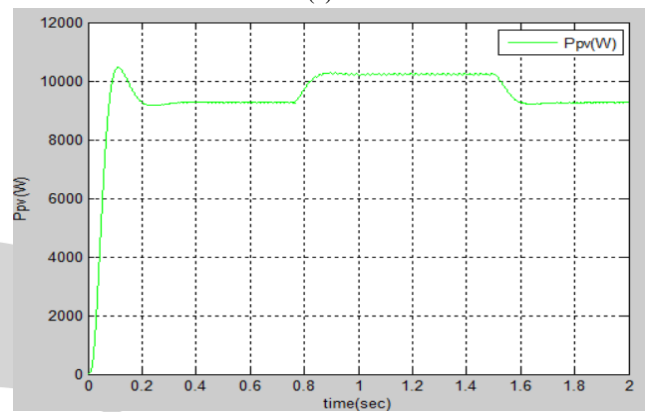
(g)



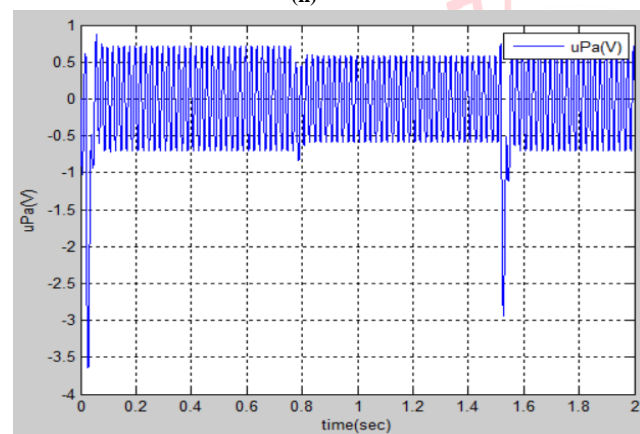
(k)



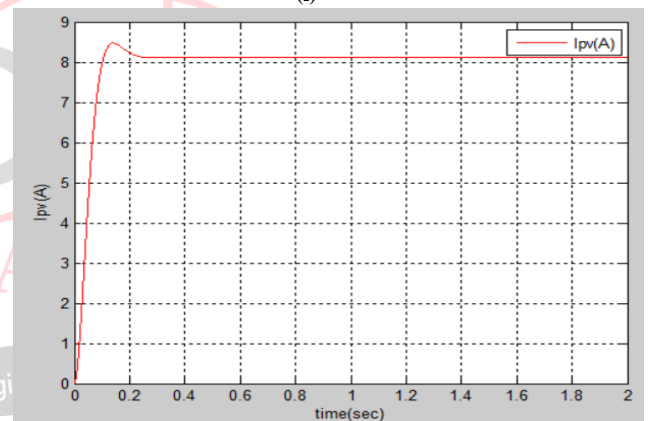
(h)



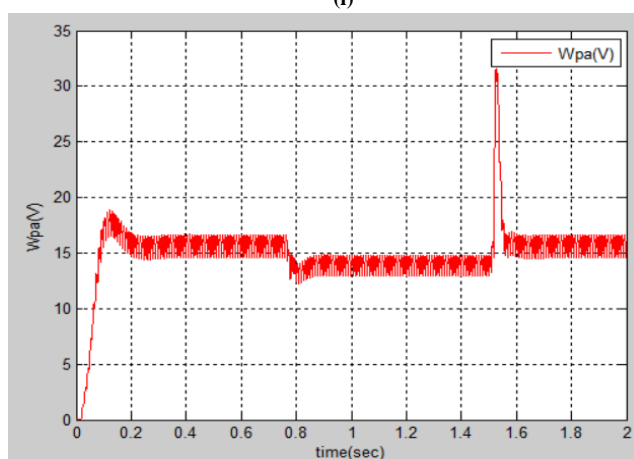
(l)



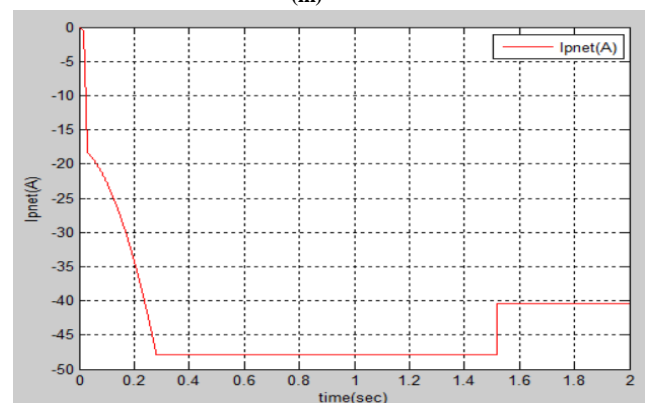
(i)



(m)



(j)



(n)

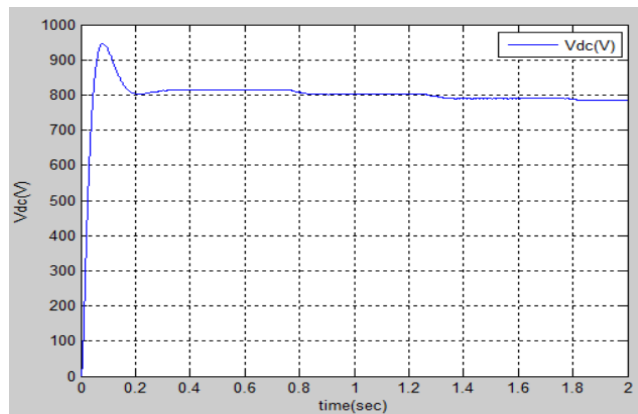
Fig.6(a-n) Load disconnection and injection condition.

'a' phase load is disconnected (Fig. 6(a-e)). The increase in  $isabc$  is observed, which accounts for the power being stored

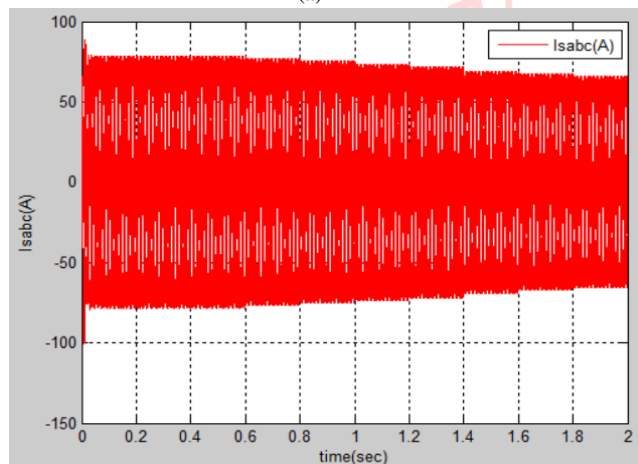
in the grid. Moreover, the control signals are observed in Fig. 6(f-n), where the change in  $I_{pnetis}$  also shown along with the other control signals. The reference and sensed grid currents obtained are sinusoidal in nature, thereby guaranteeing satisfactory performance.

### B. Changing Solar Insolation

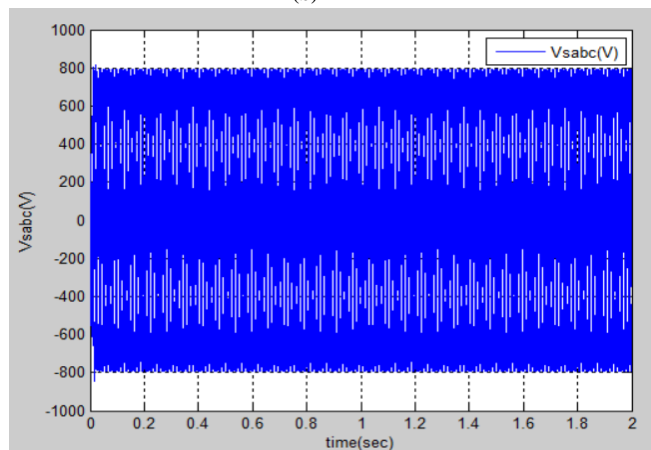
In Figs. 7(a-e), the solar insolation is varied from 1000 W/m<sup>2</sup> to 800 W/m<sup>2</sup> and ultimately 600 W/m<sup>2</sup>. The grid currents during this condition, are observed in Figs. 7(a-e), where the total harmonic distortion (THD) is less than 5% (meeting IEEE-519 standard). Moreover, changing solar insolation is presented in Figs. 5(f-k).



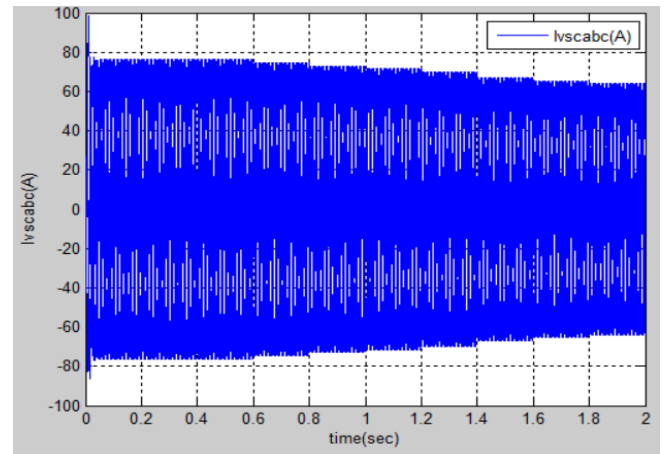
(a)



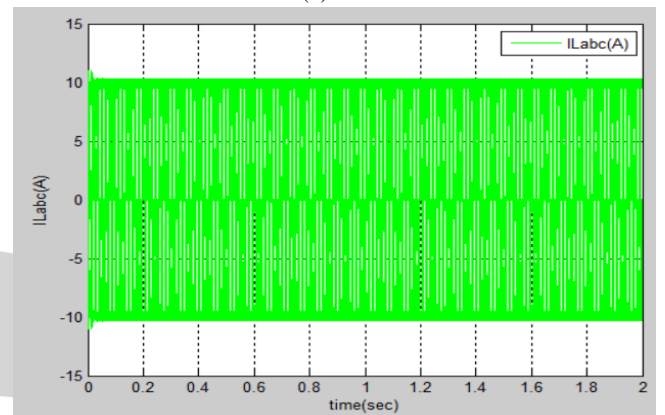
(b)



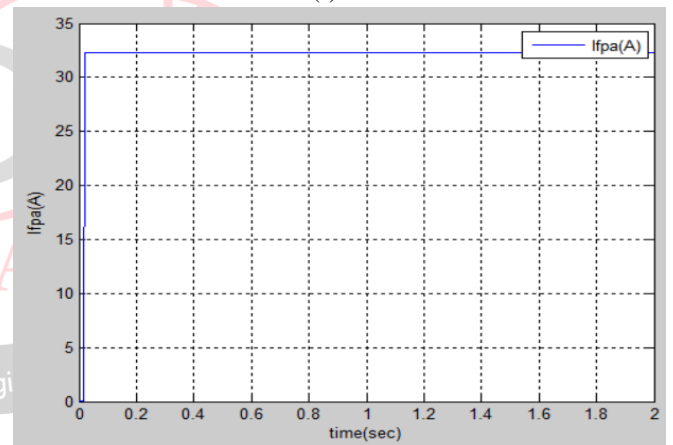
(c)



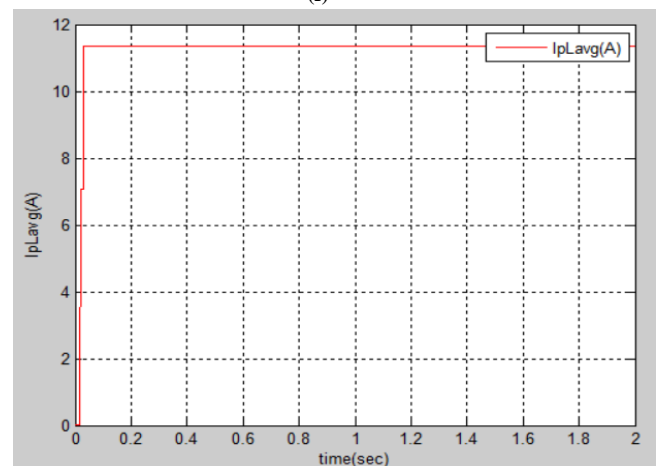
(d)



(e)



(f)



(g)

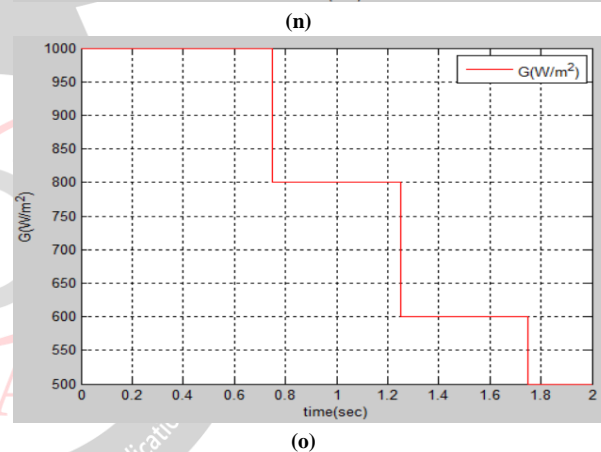
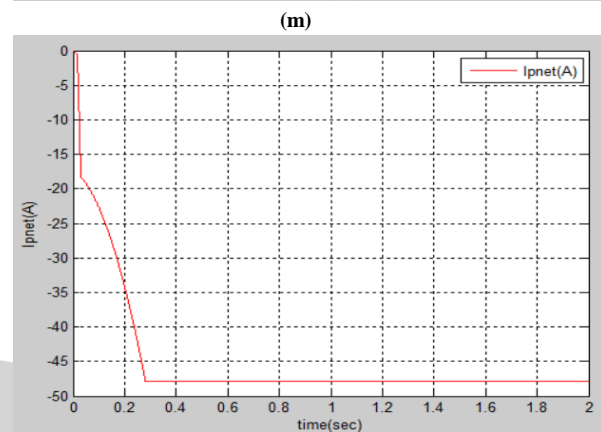
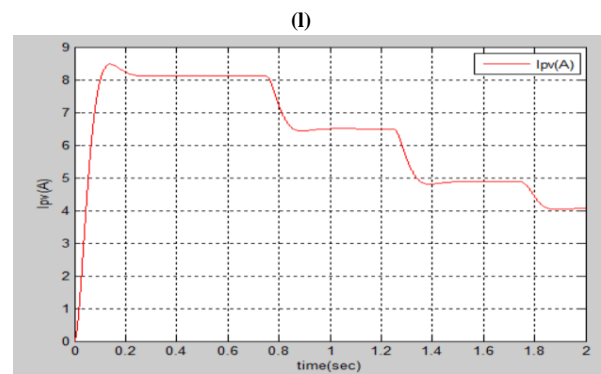
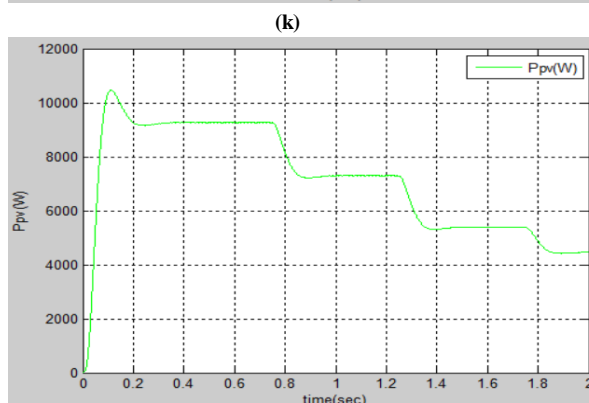
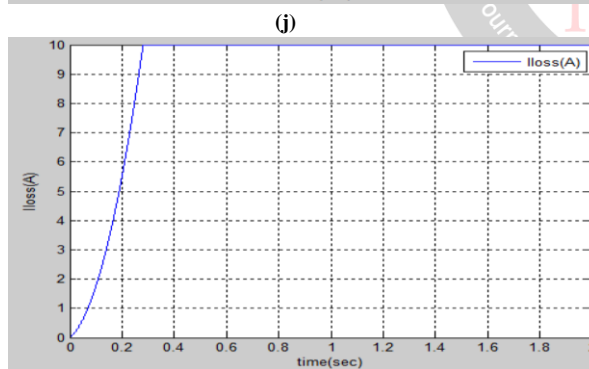
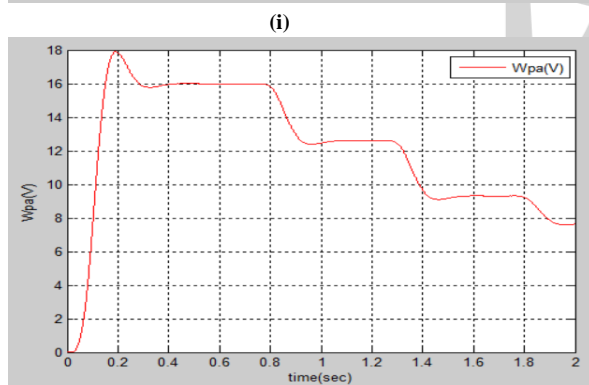
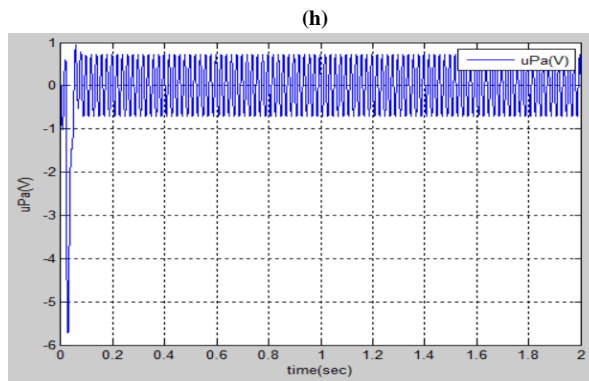
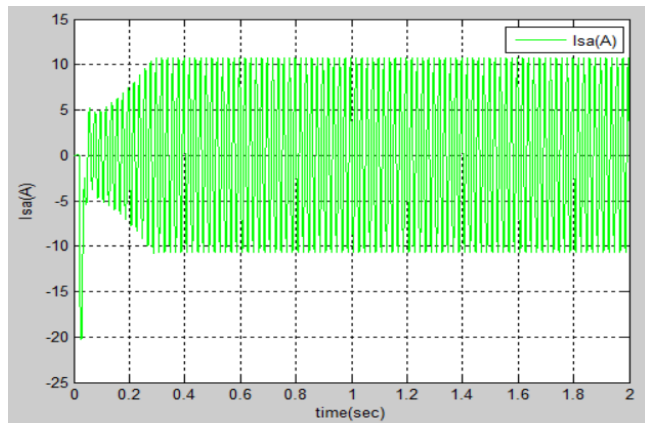


**Fig.7 (a-o) Variable insolation condition of solar PV system**  
The  $I_{pv}$  and  $P_{pv}$  are also observed during this condition. In addition, the control signals in Fig.7(l-o), such as  $w_{pv}$  and  $I_{pn}$  are observed to change in accordance with the change in solar insolation.

## VI. EDITORIAL POLICY

The grid-tied PV system's performance has been verified in weak grid conditions. Nonlinear load situations, decreased solar insolation, load injection, voltage swell and voltage sag conditions, imbalance and distortion were all tested in the lab. Even in poor grid situations like voltage sag and swell, the FOGI-FLL algorithm extracts the amplitude of the fundamental component of load currents. Simulated findings showed improved power quality in the distribution system, including harmonics reduction, power factor correction, and load balancing under a variety of scenarios, including unbalanced loads and fluctuating insolation. The solar PV feed-forward tem is incorporated into the control algorithm, reducing grid current oscillations

caused by changes in solar power generation and PCC point voltage. The system's power quality improved satisfactorily under various steady-state and dynamic settings, including load unbalancing, fluctuating insolation, and PV to DATACOM mode voltage sag, according to test results. Furthermore, when compared to a double stage architecture, test results show that a single stage topology has a higher efficiency due to lower loss. Grid current THDs are found to be under an IEEE 519 standard limit.

## REFERENCES

- [1] H. M. Bilal and A. Z. Khan, "Economic planning of network for integration of renewable: A review," *Proc. Pow. Gen. Sys. Renew. Ener. Tech. (PGSRET)*, pp. 1-3, 2015.
- [2] I. Akhtar, S. Kirmani and M. Jamil, "Analysis and design of a sustainable microgrid primarily powered by renewable energy sources with dynamic performance improvement," *IET Renew. Pow. Gen.*, vol. 13, no. 7, pp. 1024-1036, 2019.
- [3] X. Liang, "Emerging Power Quality Challenges Due to Integration of Renewable Energy Sources," *IEEE Trans. Indus. Appl.*, vol. 53, no. 2, pp. 855-866, March-April 2017.
- [4] M. D'Antonio, C. Shi, B. Wu and A. Khaligh, "Design and Optimization of a Solar Power Conversion System for Space Applications," *IEEE Trans. Indus. Appl.*, vol. 55, no. 3, pp. 2310-2319, May-June 2019.
- [5] K. R. Sree, A. K. Rathore, E. Breaz and F. Gao, "Soft-Switching Non- Isolated Current-Fed Inverter for PV/Fuel Cell Applications," *IEEE Trans. Indus. Appl.*, vol. 52, no. 1, pp. 351-359, Jan.-Feb. 2016.
- [6] P. Sreekumar and V. Khadkikar, "Adaptive Power Management Strategy for Effective Volt-Ampere Utilization of a Photovoltaic Generation Unit in Standalone Microgrids," *IEEE Trans. Indus. Appl.*, vol. 54, no. 2, pp. 1784-1792, March-April 2018.
- [7] M. N. Arafat, S. Palle, Y. Sozer and I. Husain, "Transition Control Strategy Between Standalone and Grid-Connected Operations of Voltage-Source Inverters," *IEEE Trans. Indus. Appl.*, vol. 48, no. 5, pp. 1516-1525, Sept.-Oct. 2012.
- [8] M. Farhadi and O. Mohammed, "Energy Storage Technologies for High-Power Applications," *IEEE Trans. Indus. Appl.*, vol. 52, no. 3, pp. 1953-1961, May-June 2016.
- [9] T. Wu, C. Chang, L. Lin and C. Kuo, "Power Loss Comparison of Single- and Two-Stage Grid-Connected Photovoltaic Systems," *IEEE Trans. Energy Conv.*, vol. 26, no. 2, pp. 707-715, June 2011.
- [10] O. C. Montero-Hernandez and P. N. Enjeti, "A fast detection algorithm suitable for mitigation of numerous power quality disturbances," *IEEE Trans. Indus. Appl.*, vol. 41, no. 6, pp. 1684-1690, Nov.-Dec. 2005.
- [11] T. Ma, M. H. Cintuglu and O. A. Mohammed, "Control of a Hybrid AC/DC Microgrid Involving Energy Storage and Pulsed Loads," *IEEE Trans. Indus. Appl.*, vol. 53, no. 1, pp. 567-575, Jan.-Feb. 2017.
- [12] F. Hafiz, A. R. de Queiroz and I. Husain, "Coordinated Control of PEV and PV-Based Storages in Residential Systems Under Generation and Load Uncertainties," *IEEE Trans. Indus. Appl.*, vol. 55, no. 6, pp. 5524-5532, Nov.-Dec. 2019.
- [13] F. E. Alfari and S. Bhattacharya, "Control and Real-Time Validation for Convertible Static Transmission Controller Enabled Dual Active Power Filters and PV Integration," *IEEE Trans. Indus. Appl.*, vol. 55, no. 4, pp. 4309-4320, July-Aug. 2019.
- [14] S. Al-Gahtani and R. M. Nelms, "A Modified IRPT Control Method for a Shunt Active Power Filter for Unbalanced Conditions," *Proc. IEEE Int. Symp. Indus. Electr. (ISIE)*, pp. 720-727, 2019.
- [15] W. Hernandez, M. E. Dominguez and G. Sansigre, "Analysis of the Error Signal of the LMS Algorithm," *IEEE Sig. Process. Letters*, vol. 17, no. 3, pp. 229-232, March 2010.
- [16] B. Singh, C. Jain and S. Goel, "ILST Control Algorithm of Single-Stage Dual Purpose Grid Connected Solar PV System," *IEEE Trans. Power Electr.*, vol. 29, no. 10, pp. 5347-5357, Oct. 2014.
- [17] Y. F. Wang and Y. W. Li, "Three-Phase Cascaded Delayed Signal Cancellation PLL for Fast Selective Harmonic Detection," *IEEE Trans. Indus. Electr.*, vol. 60, no. 4, pp. 1452-1463, April 2013.
- [18] Z. Xin, X. Wang, Z. Qin, M. Lu, P. C. Loh and F. Blaabjerg, "An Improved Second-Order Generalized Integrator Based Quadrature Signal Generator," *IEEE Trans. Pow. Electr.*, vol. 31, no. 12, pp. 8068-8073, Dec. 2016.
- [19] L. Asiminoael, F. Blaabjerg and S. Hansen, "Detection is key - Harmonic detection methods for active power filter applications," *IEEE Indus. Appl. Mag.*, vol. 13, no. 4, pp. 22-33, July-Aug. 2007.
- [20] Xinghuo Yu, M. O. Efe and O. Kaynak, "A general backpropagation algorithm for feedforward neural networks learning," *IEEE Trans. Neural Netw.*, vol. 13, no. 1, pp. 251-254, Jan. 2002.
- [21] O. De Jesus and M. T. Hagan, "Backpropagation Algorithms for a Broad Class of Dynamic Networks,"

- IEEE Trans. Neural Netw., vol. 18, no. 1, pp. 14-27, Jan. 2007.
- [22] P. Shukl and B. Singh, "Recursive Digital Filter Based Control for Power Quality Improvement of Grid Tied Solar PV System," Proc. IEEE India Int. Conf. Pow. Electr. (IICPE), pp. 1-6, 2018.
- [23] S. J. Darak, V. A. Prasad and E. M. - Lai, "Efficient Implementation of Reconfigurable Warped Digital Filters With Variable Low-Pass, High-Pass, Bandpass, and Bandstop Responses," IEEE Trans. Very Large Scale Int. (VLSI) Syst., vol. 21, no. 6, pp. 1165-1169, June 2013.
- [24] A. Al-Diab and C. Sourkounis, "Variable step size P&O MPPT algorithm for PV systems," Proc. Int. Conf. Opt. Elect. Electr. Equip., pp. 1097-1102, 2010.
- [25] C. Hua and Y. Chen, "Modified perturb and observe MPPT with zero oscillation in steady-state for PV systems under partial shaded conditions," Proc. IEEE Conf. Ener. Conv. (CENCON), pp. 5-9, 2017.
- [26] B. Singh, Chandra, and K. Al-Hadad, 'Power Quality: Problems and Mitigation Techniques', John Wiley & Sons Ltd., U. K., 2015.

#### AUTHORS PROFILE



D. Anusha is an Under Graduate student studying IV B.Tech Electrical and Electronics Engineering from JNTU Anantapur at Chadalawada Ramanamma Engineering College (Autonomous), Tirupati, Andhra Pradesh, India.

Her areas of interest power system and power electronics.



Dr. J. Srinu Naick received his B.E degree in Electrical & Electronics Engineering from Andhra University Vishakhapatnam AP, India in 2003 and M.Tech with Energetics from NIT Calicut, Calicut, and Kerala, India in 2007.

Ph.D with power system from Achiryanagarjuna university in 2019 He is having 17 years of teaching and research experience. He is currently working as Professor in the Department of EEE, Chadalawada Ramanamma Engineering college (Autonomous), JNTUA, Tirupati, Andhra Pradesh, India. His areas of interest are in the Power systems Industrial Drives & FACTS Controllers.